Journal of Insect Science, (2020) 20(5): 2; 1–10
doi: 10.1093/jisesa/ieaa087
Research

Identification and Expression Profiles of 14 Odorant-Binding Protein Genes From *Pieris rapae* (Lepidoptera: Pieridae)

Mao-Ye Li,[1,*] Xiu-Yun Jiang,[1,*] Yu-Zhe Qi,[1] Yuan-Jie Huang,[2] Shi-Guang Li,[1] and Su Liu[1,3,]

[1]Anhui Province Key Laboratory of Integrated Pest Management on Crops, Key Laboratory of Biology and Sustainable Management of Plant Diseases and Pests of Anhui Higher Education Institutes, College of Plant Protection, Anhui Agricultural University, 130 West Changjiang Road, Hefei, Anhui 230036, China, [2]People's Government of Fenshui Town, Tonglu County, Hangzhou 311519, China, [3]Corresponding author, e-mail: suliu@ahau.edu.cn

[*]These authors contributed equally to this work.

Subject Editor: Jurgen Ziesmann

Received 30 May 2020; Editorial decision 21 July 2020

Abstract

The small white butterfly, *Pieris rapae* (L.), is an important insect pest of *Brassica* crops. This species utilize olfactory cues to find their hosts and mates. However, the molecular mechanism underlying the olfactory perception in this species remains unclear. Here, we identified 14 odorant-binding proteins (OBP) genes—essential for insect olfaction—in *P. rapae* by exploring a previously published transcriptome dataset. Proteins encoded by all of these genes contain N-terminal signal peptides and six positionally conserved cysteine residues, which are characteristic of insect OBPs. These OBPs displayed high amino acid identity with their respective orthologs in other lepidopterans, and several conserved motifs were identified within these OBPs. Phylogenetic analysis showed that these OBPs were well segregated from each other and clustered into different branches. PrapOBP1 and PrapOBP2 were clustered into the 'general odorant-binding protein' clade, and PrapOBP3 and PrapOBP4 fall into the 'pheromone-binding protein' clade. The 14 *OBP* genes were located on seven genomic scaffolds. Of these, *PrapOBP1*, *2*, *3*, and *4* were located on scaffold332, whereas *PrapOBP5*, *6*, *7*, *8*, and *9* were located on scaffold116. Ten of the 14 genes had antenna-biased expression. Of these, *PrapOBP1*, *2*, *4*, and *13* were enriched in male antennae, whereas *PrapOBP7* and *PrapOBP10* were female-biased. Our findings suggest that these OBPs may be involved in olfactory communication. To the best of our knowledge, this is the first report on the identification and characterization of *OBP*s in *P. rapae*, and our findings provide a solid foundation for studying the functions of these genes.

Key words: small white butterfly, OBP, olfaction, genomic distribution, expression pattern

Odorant-binding proteins (OBPs) are a class of small, water-soluble proteins that play a critical role in olfaction in various insect species (Pelosi et al. 2018, Sun et al. 2018). According to a proposed model for insect olfactory process, odorants enter the antennal sensilla through small pores in the sensillar wall and bind to OBPs; then, OBPs transport these hydrophobic compounds through the aqueous sensillum lymph to reach specific odorant receptors (ORs) located in the dendritic membrane of the olfactory sensory neurons (Leal 2013, Fleischer et al. 2018). Thus, the recognition of odorants by OBPs was considered to be the initial step in olfactory perception (Vogt et al. 1985, Brito et al. 2016).

The first OBP was identified in the wild silk moth, *Antheraea polyphemus* (Cramer) (Lepidoptera: Saturniidae) and was named as pheromone-binding protein (PBP) owing to its pheromone-binding function (Vogt and Riddiford 1981). Since then, a growing number of *OBP* genes and proteins have been identified from various insect species, and their functions in odorant detection have been elucidated (Pelosi et al. 2014). In lepidopteran insects, there are two subgroups of OBPs: PBP and general odorant-binding protein (GOBP) (Vogt et al. 2015). The PBPs are believed to recognize the pheromone constituents, whereas members in the GOBP group are considered to recognize 'general' odorants such as host plant volatiles (Zhou 2010). However, many studies have also demonstrated that PBPs are able to recognize volatiles from host plants and GOBPs have a strong affinity for sex pheromone constituents (Liu et al. 2015a, Khuhro et al. 2017, Yu et al. 2018, Sun et al. 2019). PBPs and GOBPs are both belong to 'classic OBP' group, and the remarkable feature of classic OBPs is the presence of six positionally conserved cysteine residues (Zhou 2010, Pelosi et al. 2014, Brito et al. 2016). Crystal structure studies have revealed that the six cysteines form three disulfide bridges, which are essential for the protein stability (Sandler et al. 2000, Li et al. 2014, Pelosi et al. 2018). Besides classic OBPs,

there are other OBP groups with divergent cysteine motif, including plus-C OBPs (having two additional conserved cysteines plus one proline), minus-C OBPs (lost two conserved cysteines), dimer OBPs (having two six-cysteine motifs), and atypical OBPs (having 9 or 10 cysteines and a long C-terminus) (Zhou 2010).

Because OBPs are critical for insect olfaction, they have been used in the reverse chemical ecology approach to screen natural or synthetic attractants (Leal et al. 2008, Kröber et al. 2018, Venthur and Zhou 2018). For instance, two active attractants (trimethylamine and nonanal) for the mosquito *Culex quinquefasciatus* Say (Diptera: Culicidae) have been identified by using an OBP (CquiOBP1; Leal et al. 2008), and effective repellents have been discovered for *Anopheles gambiae* Giles (Diptera: Culicidae) by using the same approach (Kröber et al. 2018). In addition, OBP-based high-throughput screening of behaviorally active semiochemicals was successfully performed for *Bactrocera dorsalis* (Hendel) (Diptera: Tephritidae) (Jayanthi et al. 2014). Recently, OBPs are considered potential molecular targets for developing RNA interference (RNAi)- and genome editing-based strategies for pest management. For instance, knockdown of *OBP* genes by RNAi impairs olfactory sensitivity in *Adelphocoris lineolatus* (Goeze) (Hemiptera: Miridae) and *Helicoverpa armigera* (Hübner) (Lepidoptera: Noctuidae) (Dong et al. 2017, Zhang et al. 2017), and deletion of *OBP*s by CRISPR/Cas9 technology significantly reduces the olfactory response in *H. armigera* and *Spodoptera litura* Fabricius (Lepidoptera: Noctuidae) (Ye et al. 2017, Zhu et al. 2019).

The small white butterfly, *Pieris rapae* (L.), is a worldwide pest that infests cruciferous vegetables (Huang et al. 2018b). Outbreak populations of this insect pest can completely consume all the leaves on a Brassicaceae plant, thereby causing a significant loss in yield (Kingsolver 2000). *Pieris rapae* can be controlled with large doses of chemical pesticides; however, this practice often leads to insecticide resistance in this pest (Peng et al. 1996). Furthermore, the extensive spraying of insecticides leaves pesticide residues on the crops and pollutes the environment (Liu et al. 2014). In this case, non-insecticidal methods must urgently be developed to control *P. rapae*. Previous studies indicated that olfactory cues are essential for host and mate recognition in *P. rapae* (Renwick et al. 1992, Sato et al. 1999, McQueen and Morehouse 2018). Therefore, study of OBPs—the key proteins in the olfactory process—will not only benefit the screening of attractants and repellents for *P. rapae*, but also contribute to the development of RNAi- and CRISPR/Cas9-based methods to block the communication between *P. rapae* and their hosts and mates, thus providing promising alternatives to chemical control. However, there is limited information on the *OBP* genes underlying odorant detection in *P. rapae*. In the present study, we searched a previously published transcriptome dataset and identified 14 *OBP*s in this insect species. We analyzed the sequence characteristics, motif patterns, exon–intron structure, genomic location, and expression profiles of these genes. We found that several of these genes are predominantly expressed in the antennae, suggesting their involvement in olfaction. To the best of our knowledge, this is the first report on the identification of *OBP* genes in *P. rapae*, and the results provide a solid foundation for the functional study of these genes.

Materials and Methods

Insects

The *P. rapae* individuals used in this study were reared in our laboratory under the conditions of 26 ± 1°C, 65% relative humidity, and a 16:8 (L:D) h photoperiod, as described previously (Jiang et al. 2018). Two-day-old virgin adults were sampled, and different tissues were dissected, including 100 male antennae, 100 female antennae, 60 heads (without antennae; 30 from males and 30 from females, pooled together), 60 abdomens (30 from males and 30 from females, pooled together), and 200 legs (100 from males and 100 from females, pooled together). The samples were frozen in liquid nitrogen immediately and stored at –80°C until RNA extraction was carried out.

RNA Extraction and cDNA Synthesis

Total RNA was extracted using RNAiso Plus reagent (Takara, Dalian, China) following the manufacturer's protocol. Each RNA sample was treated with RNase-free DNase I (Takara, Dalian, China) to eliminate genomic DNA contamination. The quality of the RNA was determined by electrophoresis using a 1% (w/v) agarose gel, and the concentration of RNA were assessed with a NanoDrop 2000 spectrophotometer (Thermo Scientific, Wilmington, DE). First-strand cDNA was synthesized using the ReverTra Ace qPCR RT Master Mix (Toyobo, Osaka, Japan).

Identification of *OBP* Genes

OBP genes were identified from a previously published transcriptome dataset of *P. rapae* (BioProject number: PRJNA285028, available at NCBI's SRA database; Qi et al. 2016). The TBLASTN algorithm in the Basic Local Alignment Search Tool (BLAST) program was used for the search (Altschul et al. 1997). The annotated OBP protein sequences from other lepidopteran species, including *Danaus plexippus* (L.) (Lepidoptera: Nymphalidae), *Heliconius melpomene* L. (Lepidoptera: Nymphalidae), *Bombyx mori* (L.) (Lepidoptera: Bombycidae), *H. armigera*, *Manduca sexta* (L.) (Lepidoptera: Sphingidae), *C. suppressalis*, *Plutella xylostella* L. (Lepidoptera: Plutellidae), and *S. littoralis* (Boisduval) (Lepidoptera: Noctuidae), were used as queries. The cutoff e-value was set as 10^{-5}. All the output *OBP* sequences were manually checked, and duplicate and redundant candidates were removed. To confirm that these transcripts are not chimeric, gene-specific primers (Supp Table S1 [online only]) were designed and used to amplify full or near-full open reading frames (ORFs) from the antennal cDNA of *P. rapae*. Polymerase chain reaction (PCR) products were cloned into pMD18-T vector (Takara, Dalian, China) and sequenced.

Bioinformatic Analyses

Searching for orthologs was performed using BLASTX online program (https://blast.ncbi.nlm.nih.gov/Blast.cgi). The theoretical molecular weight (Mw) and isoelectric point (pI) were obtained using an ExPASy tool (http://web.expasy.org/compute_pi/). Putative signal peptides were predicted with SignalP 5.0 (http://www.cbs.dtu.dk/services/SignalP). Multiple alignment of OBP protein sequences was performed using Clustal Omega (http://www.ebi.ac.uk/tools/msa/clustalo/). Phylogenetic trees were constructed in MEGA7 software using the neighbor-joining method with 1,000-fold bootstrap resampling (Kumar et al. 2016). The GenBank accession numbers of the OBP protein sequences used in the phylogenetic analysis are listed in Supp Table S2 (online only). Motif pattern analysis was performed using the online program MEME (http://meme-suite.org/tools/meme); the lepidopteran OBPs used in this analysis are listed in Supp Table S3 (online only). The parameters were as follows: minimum width = 6, maximum width = 10, and maximum number of motifs to find = 8. Genomic localization and exon–intron structure of each *OBP* gene was analyzed by mapping cDNA with the *P. rapae* genomic DNA (Shen et al. 2016) using the Splign program (https://www.ncbi.nlm.nih.gov/sutils/splign/splign.cgi).

Quantitative Reverse Transcription-PCR

Quantitative reverse transcription-PCR (qRT-PCR) was carried out using SYBR Green Real-time PCR Master Mix (Toyobo, Osaka, Japan). Each reaction mixture (20 µl) contained 10 µl SYBR Green Master Mix, 1 µl (10 ng) cDNA template, 0.4 µl (0.2 µM) of each primer, and 8.2 µl nuclease-free water. Primers for qRT-PCR are listed in Supp Table S1 (online only). *18S rRNA* was used as the internal reference. The amplification efficiencies of all the primers range between 90 and 110%. Reactions were performed in 96-well plates in a CFX96 Real-time System (Bio-Rad, Hercules, CA). The thermal cycle parameters are: one cycle of 95°C for 2 min, followed by 40 cycles of 95°C for 5 s and 60°C for 25 s. To confirm that only a single gene was amplified, a heat dissociation protocol was set at the end of each thermal cycle. A no-template control and no-reverse-transcriptase control were both included on each reaction plate to detect possible contamination. The qRT-PCR reactions were performed in three biological replicates, each with three technical replicates. Relative expression levels of genes were calculated using the $2^{-\Delta CT}$ method (Livak and Schmittgen 2001).

Statistical Analysis

Data were analyzed using Data Processing System (DPS) software (version 9.5; Tang and Zhang 2013). To analyze the differences in gene expression levels among multiple samples, one-way analysis of variance (ANOVA) with Tukey's post-hoc test were performed. The level of significance was set at $P < 0.05$.

Results

Identification of *OBP* Genes in *P. rapae*

By searching the *P. rapae* transcriptome dataset, we identified 14 putative *OBP*s (*PrapOBP1* to *PrapOBP14*; Table 1). The names of these genes have been designated according to the order of discovery. These sequences were verified by PCR amplification and DNA sequencing (data not shown). All of the *OBP* genes had complete ORFs, and the length of the deduced proteins ranged from 130 to 188 amino acid residues (Table 1). The predicted Mw of these proteins ranged from 14.5 to 21.9 kDa, and the pI ranged from 4.5 to 8.8 (Table 1). BLASTX results showed that these *OBP*s shared 45–87% amino acid identities with their respective orthologs from other lepidopteran species (Table 1). The percentage of amino acid identity among all *P. rapae* OBPs ranged between 11% and 46% (Supp Table S4 [online only]). Signal peptide regions were predicted to be at the N-terminus of all the deduced PrapOBP protein sequences, and six positionally conserved cysteine residues were present in all the deduced proteins (Fig. 1). In addition, the cysteines patterns of the 14 PrapOBPs are C_1–X_{25-44}–C_2–X_3–C_3–X_{36-43}–C_4–X_{8-19}–C_5–X_8–C_6 (X represents any amino acid), indicating these proteins are classic OBPs (Fig. 1).

Phylogenetic Analysis

To better understand the relationship between the *P. rapae* OBPs and OBPs from other lepidopteran species, we performed a phylogenetic analysis (Fig. 2). The phylogeny of OBPs in this study is consistent with the findings reported by Vogt et al. (2015). In this tree, PrapOBP1 and PrapOBP2 were clustered into the GOBP1 and GOBP2 clades, respectively (Fig. 2), it is possible that the two proteins may be potential GOBPs. PrapOBP3 fall into the PBP-D clade and PrapOBP4 into PBP-C clade, implying that these proteins may belong to PBP group (Fig. 2). Other PrapOBPs were well segregated

Table 1. Information on *OBP* genes identified in *Pieris rapae*

Gene name	GenBank acc. no.	ORF (aa)	SP (aa)	Mw (kDa)	pI	BLASTX best hit				Genomic information			
						Protein name/species	GenBank acc. no.	E-value	Identity (%)	Locus	Start/stop position	Gene length (bp)	No. of exon
PrapOBP1	MT468344	162	18	18.9	5.0	GOBP1 (*Sitotroga cerealella*)	AII15787	7e-82	70	Scaffold332 (+)	332926...335846	2921	3
PrapOBP2	MT468345	163	22	18.4	5.0	GOBP2 (*Dendrolimus kikuchii*)	AGJ83353	8e-87	77	Scaffold332 (–)	223453...221888	1566	3
PrapOBP3	MT468346	166	24	19.2	5.2	PBP (*Eogystia hippophaecolus*)	AOG12882	3e-79	64	Scaffold332 (+)	212335...213911	1577	3
PrapOBP4	MT468347	161	19	18.2	5.4	PBP (*Eogystia hippophaecolus*)	AOG12880	8e-69	78	Scaffold332 (–)	217749...216520	1230	3
PrapOBP5	MT468348	151	21	16.9	5.7	OBP (*Danaus plexippus*)	OWR44714	7e-66	88	Scaffold116 (+)	150955...152386	1432	4
PrapOBP6	MT468349	149	21	16.6	5.0	OBP6 (*Spodoptera exigua*)	AGH70102	2e-33	62	Scaffold116 (–)	154730...153055	1676	4
PrapOBP7	MT468350	141	20	16.4	8.8	OBP1 (*Cnaphalocrocis medinalis*)	AFG72998	8e-80	76	Scaffold116 (–)	166978...164936	2043	5
PrapOBP8	MT468351	140	19	15.8	8.1	OBP15 (*Ectropis obliqua*)	ALS03863	2e-74	76	Scaffold116 (+)	168842...170559	1718	5
PrapOBP9	MT468352	148	20	16.5	5.3	OBP4 (*Danaus plexippus*)	OWR42852	4e-45	54	Scaffold116 (+)	171767...174697	2931	5
PrapOBP10	MT468353	130	15	14.5	4.5	OBP (*Chilo suppressalis*)	AGM38607	2e-64	71	Scaffold240 (–)	8865...8473	393	1
PrapOBP11	MT468354	188	17	21.9	5.3	OBP2 (*Danaus plexippus*)	OWR44192	6e-101	80	Scaffold1007 (–)	110625...110059	567	1
PrapOBP12	MT468355	158	18	18.2	4.9	OBP5 (*Manduca sexta*)	AAL60423	4e-43	45	Scaffold51 (+)	41221...42045	825	4
PrapOBP13	MT468356	180	21	20.4	6.0	OBP24 (*Spodoptera exigua*)	AKT26501	2e-112	87	Scaffold569 (+)	184246...198616	14371	6
PrapOBP14	MT468357	140	16	16.2	4.5	OBP (*Eogystia hippophaecolus*)	AOG12878	7e-72	83	Scaffold283 (+)	2773721...2777312	3592	5

aa: amino acid residues; SP: signal peptide; Mw: molecular weight; pI: isoelectric point. (+) and (–) represent the sense and antisense orientation in the genome scaffold, respectively.

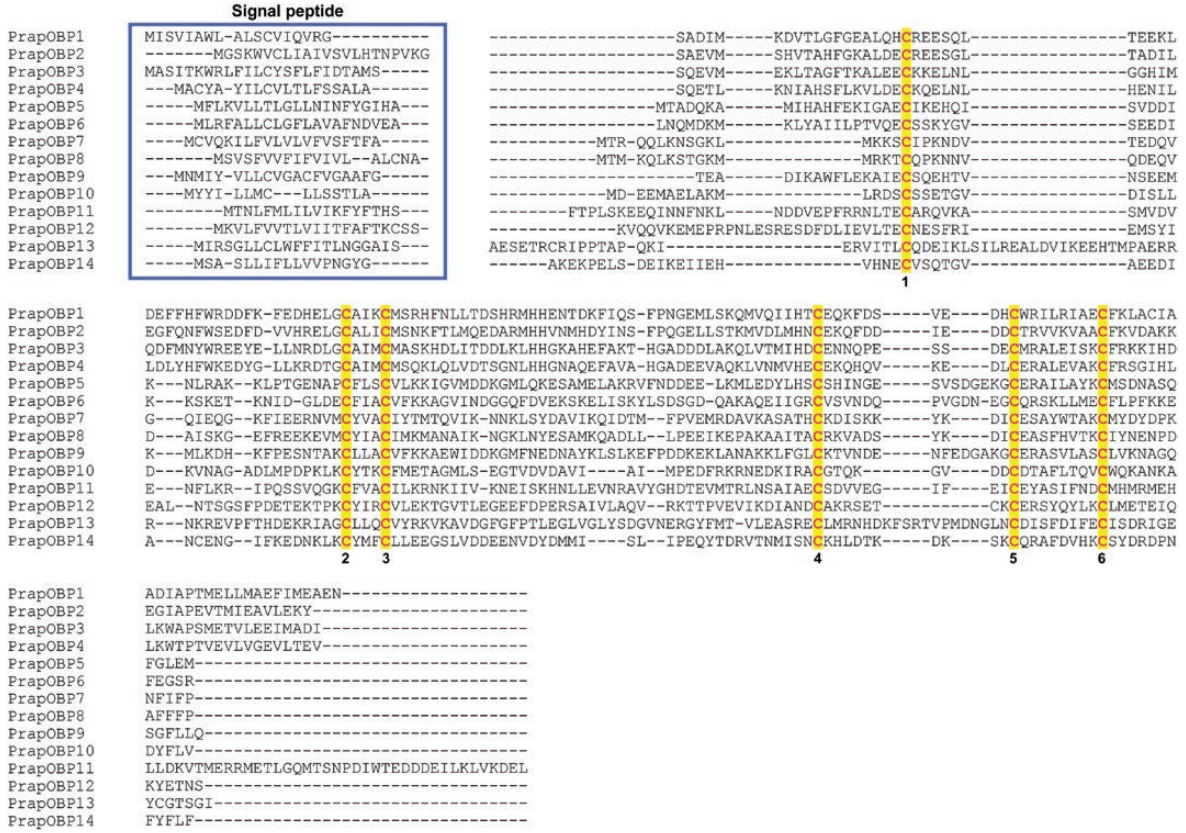

Fig. 1. Alignment of deduced protein sequences of odorant-binding proteins (OBPs) identified in *Pieris rapae*. The predicted signal peptides are depicted separately from the native proteins and marked with a blue box. Six positionally conserved cysteine residues are highlighted in red and marked with Arabic numbers 1–6.

from each other and clustered into different branches with high bootstrap support (Fig. 2).

Motif Pattern Characterization

We used the MEME program to identify the motifs of OBPs identified in *P. rapae*. Eight motifs were found by comparing the protein sequences of *P. rapae* OBPs with other lepidopteran OBPs (Fig. 3A). PrapOBP1 and PrapOBP2 (potentially GOBPs, according to phylogenetic analysis) showed the same motif pattern 4-3-1-5-6-2; PrapOBP3 was similar to PrapOBP1 and PrapOBP2 but with an additional seventh motif at its C-terminus (Fig. 3B). Surprisingly, the motif pattern differed considerably between PrapOBP3 and PrapOBP4 (two potential PBPs): PrapOBP4 lacked motif 6 compared with PrapOBP3 (which was replaced by motif 4; Fig. 3B). Among the 14 *P. rapae* OBPs, the most conserved motif pattern was 4-1-2, which was observed in six OBPs (PrapOBP5, 6, 9, 10, 12, and 14). PrapOBP7 and PrapOBP8 showed the same motif order (8-4-1-2), and PrapOBP11 and PrapOBP13 only showed the motifs 1 and 2 (Fig. 3B).

Genomic Organization and Exon–Intron Structure of *P. rapae OBP*s

We analyzed the genomic organization of *P. rapae* OBPs and found that the 14 genes were distributed among seven scaffolds (scaffold51, 116, 240, 283, 332, 569, and 1007; Table 1). Of these, *PrapOBP1*, *2*, *3*, and *4* (potentially GOBPs and PBPs) were located on scaffold332, and *PrapOBP5*, *6*, *7*, *8*, and *9* were located on scaffold116 (Table 1; Fig. 4A). The remaining five genes (*PrapOBP10*, *11*, *12*, *13*, and *14*) were located individually on a single scaffold (Table 1). Remarkably, *PrapOBP2*, *3*, and *4* were in a tight cluster spanning 11.1 kb of the genome, whereas *PrapOBP1* was located 109.5 kb downstream of *PrapOBP2* (Fig. 4A).

We also investigated the exon–intron structure of *P. rapae OBP* genes. The results showed that the size of the 14 *OBP* genes ranged from 393 to 14371 bp (Table 1). Among the 14 *OBP*s, *PrapOBP10* and *PrapOBP11* were intronless genes, whereas *PrapOBP13* contained the maximum number (six) of exons (Table 1; Fig. 4B). *PrapOBP1*, *2*, *3*, and *4* showed a common structure containing three exons and two introns; the other *OBP* genes had four or five exons (Table 1; Fig. 4B). Notably, we found that *PrapOBP1*, *2*, *3*, and *4* have conserved intron insertion sites; intron 1 was inserted between two codons, and intron 2 split a codon between nucleotides 1 and 2 (Supp Fig. S1 [online only]). Moreover, the length (181 bp) of the second exon of the four genes was equal (Supp Table S5 [online only]).

Expression Profiles of *P. rapae OBP*s

We investigated the expression profiles of *P. rapae OBP* genes in different tissues using qRT-PCR. The results showed that ten genes (*PrapOBP1*, *2*, *3*, *4*, *7*, *8*, *10*, *12*, *13*, and *14*) were specifically or mainly expressed in the antennae (Fig. 5). Of these, *PrapOBP1*, *2*, *4*, and *13* mRNAs were enriched in male antennae, whereas *PrapOBP7* and *PrapOBP10* mRNAs were enriched in female antennae. For *PrapOBP3*, *8*, *12*, and *14*, the antennal mRNA expression did not significantly differ between the two sexes ($P < 0.05$; Fig. 5). We also found that several *P. rapae OBP*s were expressed in non-olfactory

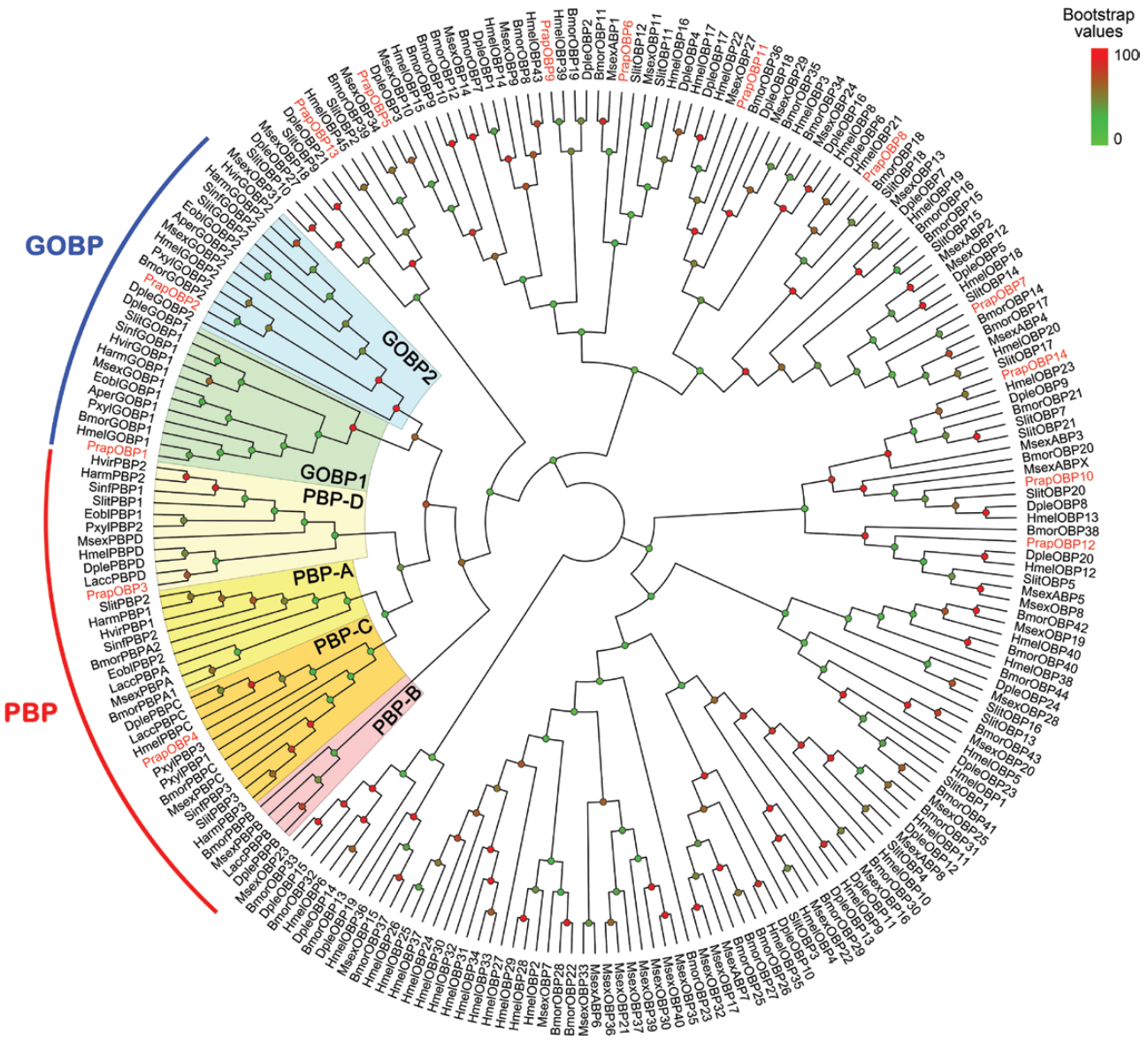

Fig. 2. Phylogenetic analysis of OBPs from *Pieris rapae* and other lepidopteran species, including *Bombyx mori* (Bmor), *Manduca sexta* (Msex), *Danaus plexippus* (Dple), *Heliconius melpomene* (Hmel), *Spodoptera littoralis* (Slit), *Helicoverpa armigera* (Harm), *Heliothis virescens* (Hvir), *Sesamia inferens* (Sinf), *Antheraea pernyi* (Aper), *Plutella xylostella* (Pxyl), *Ectropis obliqua* (Eobl), and *Lerema accius* (Lacc). The tree was constructed with MEGA7 software using the neighbor-joining method. Bootstrap values are indicated with colors ranging from green (0) to red (100). The *P. rapae* OBPs are highlighted in red. GenBank accession numbers of the OBPs used are listed in Supp Table S2 (online only).

tissues. For example, *PrapOBP5* and *PrapOBP6* were mainly expressed in the abdomen, and *PrapOBP9* and *PrapOBP11* were enriched in all the tested tissues including male and female antennae, head, abdomen, and legs (Fig. 5).

Discussion

To date, *OBP* gene families have been identified in various insect species, through genomic and/or transcriptomic analyses (reviewed by Venthur and Zhou 2018). These studies have greatly contributed to the research on the molecular mechanisms underlying insect olfaction (Venthur and Zhou 2018). However, information on the *OBP*s in *P. rapae* remains limited, which restricts the understanding of olfactory signal pathways in this insect species. In the present study, we identified 14 *OBP* genes from *P. rapae* by searching a previously published transcriptome dataset. To the best of our knowledge, this is the first report on the identification and characterization of *OBP*s in *P. rapae*, and our findings pave the way for studying of the function of these genes.

The deduced protein sequences of the *P. rapae* OBPs contain N-terminal signal peptides and six positionally conserved cysteine residues, which are the hallmark of insect OBPs (Pelosi et al. 2018, Sun et al. 2018). The motif pattern analysis showed that the motif pattern varied in different OBPs; PrapOBP1 and PrapOBP2 (two potential GOBPs) have a similar motif pattern (4-3-1-5-6-2), and they lack motif 7 at the C-terminus, unlike PrapOBP3 (potentially PBP). This difference implies a possible functional difference between them. In most lepidopterans, GOBPs and PBPs show distinct binding affinities for plant volatiles and sex pheromone constituents (Liu et al. 2015b, Khuhro et al. 2017, Huang et al. 2018a,

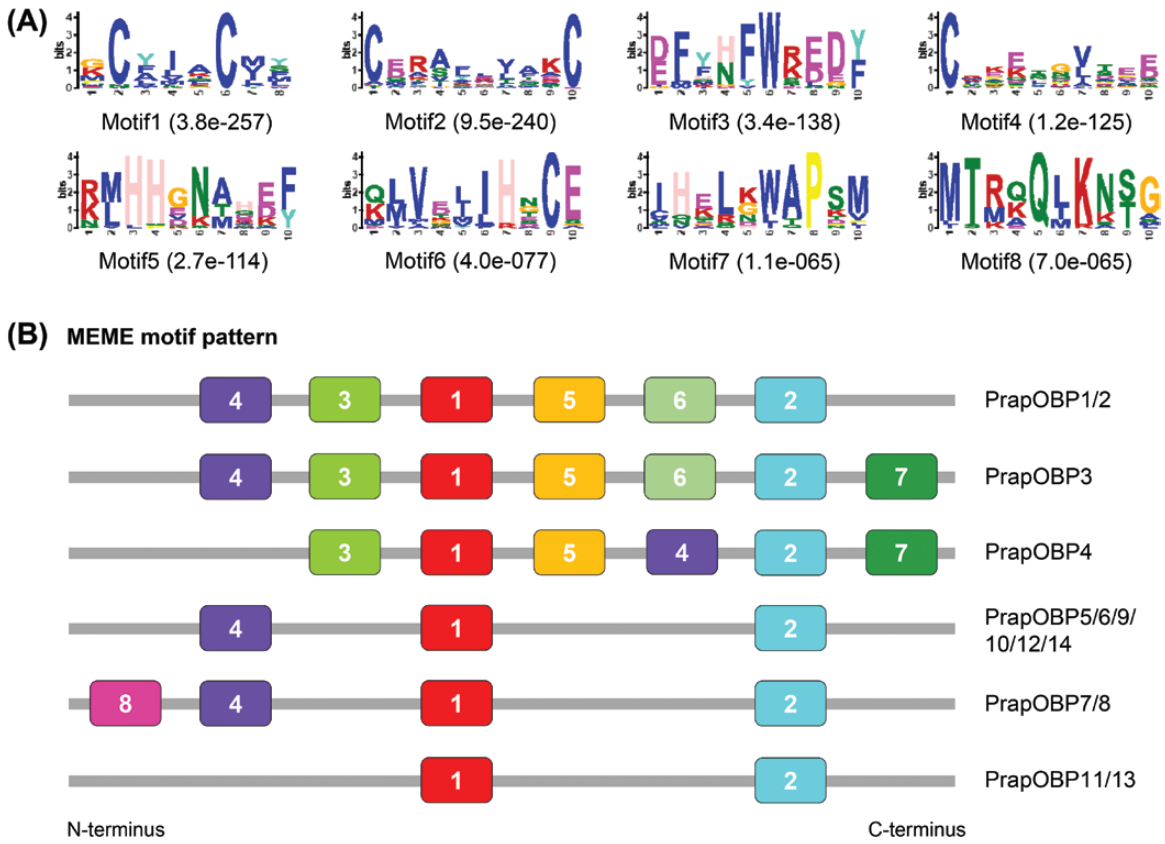

Fig. 3. Motif pattern analysis of *Pieris rapae* OBPs. (A) The eight motifs (motif1–8) identified in *P. rapae* OBPs and their homologs from other lepidopterans. The number in the parentheses indicates the expect-value (e-value) of each motif calculated by the MEME program. (B) Location of each motif in the protein sequences. The numbers in the colored boxes correspond to the numbered motifs in (A). The protein sequences of the OBPs used are listed in Supp Table S3 (online only).

Sun et al. 2019). The most noteworthy finding was that the two potential PBPs, PrapOBP3 and PrapOBP4, displayed different motif patterns. In most lepidopteran species, including *S. litura*, *Dendrolimus houi* Lajonquiere (Lepidoptera: Lasiocampidae), and *De. kikuchii* Matsumura (Lepidoptera: Lasiocampidae), the motif patterns between PBPs are quite similar (Zhang et al. 2014, Gu et al. 2015); however, in *Hyphantria cunea* (Drury) (Lepidoptera: Arctiidae), PBP1 displayed distinct motif pattern with PBP2 (Zhang et al. 2016). It is possible that PrapOBP3 and PrapOBP4 may have an affinity for different kinds of pheromone constituents and/or plant odorants. PBPs that selectively bind different types of odorants have also been reported in other moth species. For example, PBP1 in *H. armigera* strongly bind sex pheromone components, whereas PBP2 specifically binds alcohols, and PBP3 preferably binds acetates (Guo et al. 2012). A similar phenomenon was also observed in *Helicoverpa assulta* (Guenée) (Lepidoptera: Noctuidae) and *Sesamia inferens* (Walker) (Lepidoptera: Noctuidae) (Guo et al. 2012, Jin et al. 2014).

We found that several *P. rapae OBP*s were located on the same genomic scaffold and formed gene clusters, for example, *PrapOBP1*, *2*, *3*, and *4* on scaffold332, and *PrapOBP5*, *6*, *7*, *8*, and *9* on scaffold116 (Fig. 4A). This phenomenon is also observed in other insect species, such as *Drosophila melanogaster* Meigen (Diptera: Drosophilidae), *Apis mellifera* L. (Hymenoptera: Apidae), *B. mori*, and *Myzus persicae* (Sulzer) (Homoptera: Aphididae) (Hekmat-Scafe et al. 2002, Forêt and Maleszka 2006, Gong et al. 2009, Wang et al. 2019). Among insect *OBP*s, *GOBP*s and *PBP*s are lepidopteran specific, and the location of *GOBP* and *PBP* genes on the same genomic scaffold has been found in several lepidopterans, including *B. mori*, *M. sexta*, *Danaus plexippus* (L.) (Lepidoptera: Nymphalidae), and *S. frugiperda* (Smith) (Lepidoptera: Noctuidae) (Gong et al. 2009, Yasukochi et al. 2018). Vogt et al. (2015) analyzed the *GOBP* and *PBP* genes in lepidopterans and suggested that *GOBP*s and *PBP*s are derived by duplication events from a common ancestor, based on the following evidence: 1) *GOBP*s and *PBP*s contain three exons, and the length of the second exon is identical; 2) introns in *GOBP*s and *PBP*s have conserved insertion sites and phase (positioned between codons or within a codon); and 3) in the phylogenetic tree, the *PBP/GOBP* clade forms a well-supported lineage, which excludes other OBPs (Vogt et al. 2015). In the present study, we found that *PrapOBP1*, *2*, *3*, and *4* have the same exon–intron structures and share conserved intron positions (Supp Fig. S1 [online only]; Supp Table S5 [online only]), suggesting that they originated by duplication of an ancestral gene. Further analysis of the exon–intron structure in *OBP*s will provide new insights into the evolution of this gene family in *P. rapae*.

*OBP*s that are mainly expressed in the insect antennae are considered to have an olfactory function. By contrast, *OBP*s enriched in non-olfactory tissues are thought to be involved in other physiological processes (Pelosi et al. 2018). Therefore, the potential function of *OBP*s could be predicted by analyzing their expression profiles in different tissues. Our qRT-PCR results showed that ten *P. rapae OBP*s displayed antenna-specific or

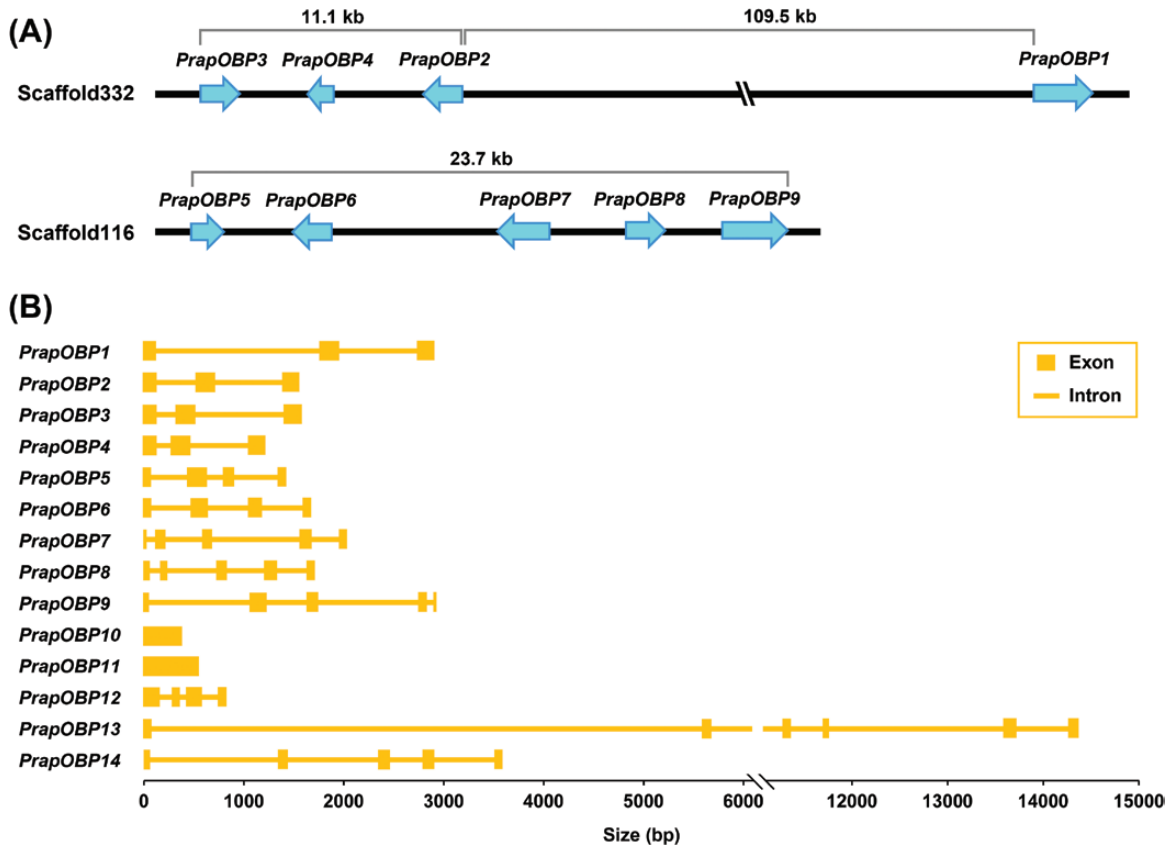

Fig. 4. Genomic location (A) and exon–intron structure (B) of *Pieris rapae OBP* genes.

antenna-enriched expression, indicating that these genes may play important roles in olfaction. Among these genes, four (*PrapOBP1*, *2*, *4*, and *13*) were mainly expressed in male antennae. These genes may encode proteins involved in the detection of sex pheromones released from females. In many other lepidopteran species such as *C. suppressalis*, *Se. inferens*, and *Agrotis ipsilon* (Hufnagel) (Lepidoptera: Noctuidae), male antenna-biased OBPs displayed a strong affinity for sex pheromone components (Gu et al. 2013, Jin et al. 2014, Chang et al. 2015). We observed that *PrapOBP7* and *PrapOBP10* showed female antenna-biased expression. Previous studies have shown that the *P. rapae* females use chemicals emitted from host plants to locate oviposition sites (Renwick et al. 1992, Sato et al. 1999). Furthermore, mate recognition behavior in *P. rapae* females largely relies on the perception of volatiles released by males (McQueen and Morehouse 2018). Thus, it is possible that *PrapOBP3* and *PrapOBP6* are involved in these female-specific functions.

We also found that *PrapOBP5* and *PrapOBP6* were enriched in the abdomen, and *PrapOBP9* and *PrapOBP11* were highly abundant in all the tested tissues, including male and female antennae, head, abdomen, and legs. These *OBP*s may have important functions in physiological pathways other than olfaction, e.g., gustatory function. In *Ad. lineolatus*, *Apolygus lucorum* (Meyer-Dür) (Heteroptera: Miridae), *Helicoverpa zea* (Boddie) (Lepidoptera: Noctuidae), and *Meteorus pulchricornis* (Wesmael) (Hymenoptera: Braconidae), a large number of *OBP*s are expressed in the mouthparts, ovipositor, and tarsi. These *OBP*s are considered to have a potential gustatory function (Sun et al. 2016, Sheng et al. 2017, Sun et al. 2017, Dou et al. 2019, Li et al. 2020). Another potential function of these genes is as transporters that bind xenobiotic compounds, especially insecticides. In *Apis cerana* Fabricius (Hymenoptera: Apidae), *Athetis lepigone* (Möschler) (Lepidoptera: Noctuidae), *Ectropis obliqua* Prout (Lepidoptera: Geometridae), and *S. litura*, OBPs can interact with various insecticides and may contribute to defense against these harmful xenobiotic compounds (Li et al. 2015, 2017; Zhang et al. 2020).

It should be noted that, although the findings discussed above lead us to predict the potential functions for *OBP*s in *P. rapae*, we measured the transcription levels of the genes in adult tissues, but did not measure the expression patterns of these genes in larval tissues. It is known that *OBP*s in larval antennae are essential for chemosensation and behavior guidance (Jin et al. 2015, Zhu et al. 2016). Determining the *OBP* expression profiles in larval tissues will provide additional supporting evidence that these genes may be playing important roles in chemosensory perception.

In conclusion, we successfully identified 14 putative *OBP*s from *P. rapae* by searching the transcriptomic dataset. Phylogeny, sequence motif, genomic localization, and expression profile analyses suggested that some of these genes are involved in olfaction. The results of this work will not only lead to a better understanding of the olfactory system in this lepidopteran species but also contribute to the development of sustainable pest management strategies using OBPs as targets to disrupt insect behavior.

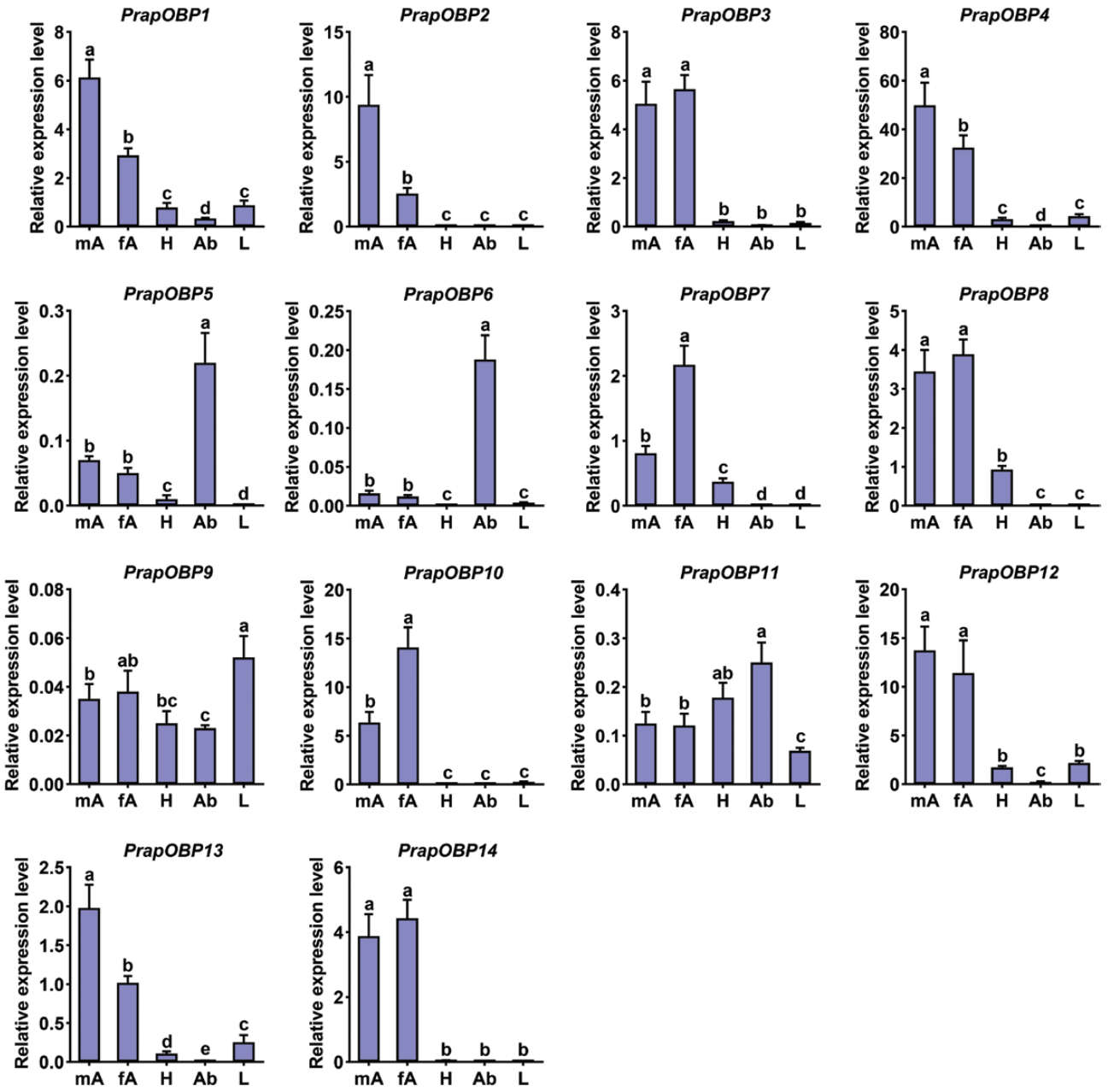

Fig. 5. Relative expression levels of *OBP* genes in different tissues of *Pieris rapae*. mA: male antennae; fA: female antennae; H: head (without antennae); Ab: abdomen; L: legs. Data are presented as mean ($n = 3$) ± SE. Different lowercase letters indicate significant differences ($P < 0.05$; one-way ANOVA with Tukey's test).

Supplementary Data

Supplementary data are available at *Journal of Insect Science* online.

Fig. S1. Alignment of amino acid sequences of four odorant-binding proteins (PrapOBP1 to PrapOBP4) from *Pieris rapae*. Signal peptides have been removed from the sequences, and six positionally conserved cysteines are highlighted in red. Two introns are identified in each gene, and the conserved intron insertion sites are marked with boxes. In each box, nucleotide sequences are in lowercase letters, followed by the respective amino acid residues (capitalized). The slash indicates the intron insertion site. Intron 1 is inserted between two codons and intron 2 splits a codon between nucleotides 1 and 2.

Acknowledgments

This research was supported by the Anhui Provincial Natural Science Foundation (grant number 1908085MC70), the Key Project of Natural Science Foundation of Universities in Anhui Province (grant number KJ2016A226), and the Key Projects of China National Tobacco Corporation Sichuan Company (grant numbers SCYC201703 and SCYC201806).

References Cited

Altschul, S. F., T. L. Madden, A. A. Schäffer, J. Zhang, Z. Zhang, W. Miller, and D. J. Lipman. 1997. Gapped BLAST and PSI-BLAST: a new generation of protein database search programs. Nucleic Acids Res. 25: 3389–3402.

Brito, N. F., M. F. Moreira, and A. C. Melo. 2016. A look inside odorant-binding proteins in insect chemoreception. J. Insect Physiol 95: 51–65.

Chang, H., Y. Liu, T. Yang, P. Pelosi, S. Dong, and G. Wang. 2015. Pheromone binding proteins enhance the sensitivity of olfactory receptors to sex pheromones in *Chilo suppressalis*. Sci. Rep 5: 13093.

Dong, K., L. Sun, J. T. Liu, S. H. Gu, J. J. Zhou, R. N. Yang, K. H. Dhiloo, X. W. Gao, Y. Y. Guo, and Y. J. Zhang. 2017. RNAi-Induced electrophysiological and behavioral changes reveal two pheromone binding

proteins of *Helicoverpa armigera* involved in the perception of the main sex pheromone component Z11-16:Ald. J. Chem. Ecol 43: 207–214.

Dou, X., S. Liu, S. J. Ahn, M. Y. Choi, and R. Jurenka. 2019. Transcriptional comparison between pheromone gland-ovipositor and tarsi in the corn earworm moth *Helicoverpa zea*. Comp. Biochem. Physiol. Part D. Genomics Proteomics D31: 100604.

Fleischer, J., P. Pregitzer, H. Breer, and J. Krieger. 2018. Access to the odor world: olfactory receptors and their role for signal transduction in insects. Cell. Mol. Life Sci 75: 485–508.

Forêt, S., and R. Maleszka. 2006. Function and evolution of a gene family encoding odorant binding-like proteins in a social insect, the honey bee (*Apis mellifera*). Genome Res. 16: 1404–1413.

Gong, D. P., H. J. Zhang, P. Zhao, Q. Y. Xia, and Z. H. Xiang. 2009. The odorant binding protein gene family from the genome of silkworm, *Bombyx mori*. BMC Genomics 10: 332.

Gu, S. H., J. J. Zhou, G. R. Wang, Y. J. Zhang, and Y. Y. Guo. 2013. Sex pheromone recognition and immunolocalization of three pheromone binding proteins in the black cutworm moth *Agrotis ipsilon*. Insect Biochem. Mol. Biol 43: 237–251.

Gu, S. H., J. J. Zhou, S. Gao, D. H. Wang, X. C. Li, Y. Y. Guo, and Y. J. Zhang. 2015. Identification and comparative expression analysis of odorant binding protein genes in the tobacco cutworm *Spodoptera litura*. Sci. Rep 5: 13800.

Guo, H., L. Q. Huang, P. Pelosi, and C. Z. Wang. 2012. Three pheromone-binding proteins help segregation between two *Helicoverpa* species utilizing the same pheromone components. Insect Biochem. Mol. Biol 42: 708–716.

Hekmat-Scafe, D. S., C. R. Scafe, A. J. McKinney, and M. A. Tanouye. 2002. Genome-wide analysis of the odorant-binding protein gene family in *Drosophila melanogaster*. Genome Res. 12: 1357–1369.

Huang, G. Z., J. T. Liu, J. J. Zhou, Q. Wang, J. Z. Dong, Y. J. Zhang, X. C. Li, J. Li, and S. H. Gu. 2018a. Expressional and functional comparisons of two general odorant binding proteins in *Agrotis ipsilon*. Insect Biochem. Mol. Biol 98: 34–47.

Huang, H.-J., T.-Q. Zhang, Q. Li, C.-X. Zhang, and B.-Q. Zhang. 2018b. Transcriptional analysis of *Pieris rapae* in response to *P. rapae* granulovirus. J. Asia Pac. Entomol 21: 513–518.

Jayanthi, K. P., V. Kempraj, R. M. Aurade, T. K. Roy, K. S. Shivashankara, and A. Verghese. 2014. Computational reverse chemical ecology: virtual screening and predicting behaviorally active semiochemicals for *Bactrocera dorsalis*. BMC Genomics 15: 209.

Jiang, X.-C., X.-Y. Jiang, and S. Liu. 2018. Molecular characterization and expression analysis of two acetylcholinesterase genes from the small white butterfly *Pieris rapae* (Lepidoptera: Pieridae). J. Insect Sci 18: 2.

Jin, J.-Y., Z.-Q. Li, Y.-N. Zhang, N.-Y. Liu, and S.-L. Dong. 2014. Different roles suggested by sex-biased expression and pheromone binding affinity among three pheromone binding proteins in the pink rice borer, *Sesamia inferens* (Walker) (Lepidoptera: Noctuidae). J. Insect Physiol 66: 71–79.

Jin, R., N.-y. Liu, Y. Liu, and S.-l. Dong. 2015. A larval specific OBP able to bind the major female sex pheromone component in *Spodoptera exigua* (Hübner). J. Integr. Agr 14: 1356–1366.

Khuhro, S. A., H. Liao, X.-T. Dong, Q. Yu, Q. Yan, and S.-L. Dong. 2017. Two general odorant binding proteins display high bindings to both host plant volatiles and sex pheromones in a pyralid moth *Chilo suppressalis* (Lepidoptera: Pyralidae). J. Asia Pac. Entomol 20: 521–528.

Kingsolver, J. G. 2000. Feeding, growth, and the thermal environment of cabbage white caterpillars, *Pieris rapae* L. Physiol. Biochem. Zool 73: 621–628.

Kröber, T., K. Koussis, M. Bourquin, P. Tsitoura, M. Konstantopoulou, T. S. Awolola, F. R. Dani, H. Qiao, P. Pelosi, K. Iatrou, et al. 2018. Odorant-binding protein-based identification of natural spatial repellents for the African malaria mosquito *Anopheles gambiae*. Insect Biochem. Mol. Biol 96: 36–50.

Kumar, S., G. Stecher, and K. Tamura. 2016. MEGA7: molecular evolutionary genetics analysis version 7.0 for bigger datasets. Mol. Biol. Evol 33: 1870–1874.

Leal, W. S. 2013. Odorant reception in insects: roles of receptors, binding proteins, and degrading enzymes. Annu. Rev. Entomol 58: 373–391.

Leal, W. S., R. M. Barbosa, W. Xu, Y. Ishida, Z. Syed, N. Latte, A. M. Chen, T. I. Morgan, A. J. Cornel, and A. Furtado. 2008. Reverse and conventional chemical ecology approaches for the development of oviposition attractants for *Culex* mosquitoes. PLoS One 3: e3045.

Li, H., A. Zhang, L. Z. Chen, G. Zhang, and M. Q. Wang. 2014. Construction and analysis of cDNA libraries from the antennae of *Batocera horsfieldi* and expression pattern of putative odorant binding proteins. J. Insect Sci 14: 57.

Li, H., F. Wu, L. Zhao, J. Tan, H. Jiang, and F. Hu. 2015. Neonicotinoid insecticide interact with honeybee odorant-binding protein: Implication for olfactory dysfunction. Int. J. Biol. Macromol 81: 624–630.

Li, H., L. Zhao, X. Fu, X. Song, F. Wu, M. Tang, H. Cui, and J. Yu. 2017. Physicochemical evidence on sublethal neonicotinoid imidacloprid interacting with an odorant-binding protein from the tea geometrid moth, *Ectropis obliqua*. J. Agric. Food Chem 65: 3276–3284.

Li, Z., Y. Zhang, X. An, Q. Wang, A. Khashaveh, S. Gu, S. Liu, and Y. Zhang. 2020. Identification of Leg Chemosensory Genes and Sensilla in the *Apolygus lucorum*. Front. Physiol 11: 276.

Liu, Y.-Q., Z.-H. Shi, M. P. Zalucki, and S.-S. Liu. 2014. Conservation biological control and IPM practices in Brassica vegetable crops in China. Biol. Control 68: 37–46.

Liu, N. Y., K. Yang, Y. Liu, W. Xu, A. Anderson, and S. L. Dong. 2015a. Two general-odorant binding proteins in *Spodoptera litura* are differentially tuned to sex pheromones and plant odorants. Comp. Biochem. Physiol. A. Mol. Integr. Physiol 180: 23–31.

Liu, N. Y., F. Yang, K. Yang, P. He, X. H. Niu, W. Xu, A. Anderson, and S. L. Dong. 2015b. Two subclasses of odorant-binding proteins in *Spodoptera exigua* display structural conservation and functional divergence. Insect Mol. Biol 24: 167–182.

Livak, K. J., and T. D. Schmittgen. 2001. Analysis of relative gene expression data using real-time quantitative PCR and the $2^{-\Delta\Delta CT}$ method. Methods 25: 402–408.

McQueen, E. W., and N. I. Morehouse. 2018. Rapid divergence of wing volatile profiles between subspecies of the butterfly *Pieris rapae* (Lepidoptera: Pieridae). J. Insect Sci 18: 33.

Pelosi, P., I. Iovinella, A. Felicioli, and F. R. Dani. 2014. Soluble proteins of chemical communication: an overview across arthropods. Front. Physiol 5: 320.

Pelosi, P., I. Iovinella, J. Zhu, G. Wang, and F. R. Dani. 2018. Beyond chemoreception: diverse tasks of soluble olfactory proteins in insects. Biol. Rev. Camb. Philos. Soc 93: 184–200.

Peng, L., R. Lin, J. Zeng, Q. Yang, and Y. Huang. 1996. Monitoring of resistance to chemicals in *Pieris rapae* and *Brevicoryne brassicae*. J. Southwest Agri. Univ 18: 530–532.

Qi, L., Q. Fang, L. Zhao, H. Xia, Y. Zhou, J. Xiao, K. Li, and G. Ye. 2016. De novo assembly and developmental transcriptome analysis of the small white butterfly *Pieris rapae*. PLoS One 11: e0159258.

Renwick, J. A. A., C. D. Radke, K. Sachdev-Gupta, and E. Städler. 1992. Leaf surface chemicals stimulating oviposition by *Pieris rapae* (Lepidoptera: Pieridae) on cabbage. Chemoecology 3: 33–38.

Sandler, B. H., L. Nikonova, W. S. Leal, and J. Clardy. 2000. Sexual attraction in the silkworm moth: structure of the pheromone-binding-protein-bombykol complex. Chem. Biol 7: 143–151.

Sato, Y., S. Yano, J. Takabayashi, and N. Ohsaki. 1999. *Pieris rapae* (Ledidoptera: Pieridae) females avoid oviposition on *Rorippa indica* plants infested by conspecific larvae. Appl. Entomol. Zool 34: 333–337.

Shen, J., Q. Cong, L. N. Kinch, D. Borek, Z. Otwinowski, and N. V. Grishin. 2016. Complete genome of *Pieris rapae*, a resilient alien, a cabbage pest, and a source of anti-cancer proteins. F1000Res 5: 2631.

Sheng, S., C. W. Liao, Y. Zheng, Y. Zhou, Y. Xu, W. M. Song, P. He, J. Zhang, and F. A. Wu. 2017. Candidate chemosensory genes identified in the endoparasitoid *Meteorus pulchricornis* (Hymenoptera: Braconidae) by antennal transcriptome analysis. Comp. Biochem. Physiol. Part D. Genomics Proteomics 22: 20–31.

Sun, L., Y. Wei, D. D. Zhang, X. Y. Ma, Y. Xiao, Y. N. Zhang, X. M. Yang, Q. Xiao, Y. Y. Guo, and Y. J. Zhang. 2016. The mouthparts enriched odorant binding protein 11 of the alfalfa plant bug *Adelphocoris lineolatus*

displays a preferential binding behavior to host plant secondary metabolites. Front. Physiol 7: 201.

Sun, L., Q. Wang, Q. Wang, K. Dong, Y. Xiao, and Y. J. Zhang. 2017. Identification and characterization of odorant binding proteins in the forelegs of *Adelphocoris lineolatus* (Goeze). Front. Physiol 8: 735.

Sun, J. S., S. Xiao, and J. R. Carlson. 2018. The diverse small proteins called odorant-binding proteins. Open Biol 8: 180208.

Sun, L., Q. Wang, Y. Zhang, X. Tu, Y. Yan, Q. Wang, K. Dong, Y. Zhang, and Q. Xiao. 2019. The sensilla trichodea-biased EoblPBP1 binds sex pheromones and green leaf volatiles in *Ectropis obliqua* Prout, a geometrid moth pest that uses Type-II sex pheromones. J. Insect Physiol 116: 17–24.

Tang, Q. Y., and C. X. Zhang. 2013. Data Processing System (DPS) software with experimental design, statistical analysis and data mining developed for use in entomological research. Insect Sci. 20: 254–260.

Venthur, H., and J. J. Zhou. 2018. Odorant receptors and odorant-binding proteins as insect pest control targets: a comparative analysis. Front. Physiol 9: 1163.

Vogt, R. G., and L. M. Riddiford. 1981. Pheromone binding and inactivation by moth antennae. Nature 293: 161–163.

Vogt, R. G., L. M. Riddiford, and G. D. Prestwich. 1985. Kinetic properties of a sex pheromone-degrading enzyme: the sensillar esterase of *Antheraea polyphemus*. Proc. Natl. Acad. Sci. U. S. A 82: 8827–8831.

Vogt, R. G., E. Große-Wilde, and J. J. Zhou. 2015. The Lepidoptera odorant binding protein gene family: gene gain and loss within the GOBP/PBP complex of moths and butterflies. Insect Biochem. Mol. Biol 62: 142–153.

Wang, Q., J. J. Zhou, J. T. Liu, G. Z. Huang, W. Y. Xu, Q. Zhang, J. L. Chen, Y. J. Zhang, X. C. Li, and S. H. Gu. 2019. Integrative transcriptomic and genomic analysis of odorant binding proteins and chemosensory proteins in aphids. Insect Mol. Biol 28: 1–22.

Yasukochi, Y., B. Yang, T. Fujimoto, K. Sahara, T. Matsuo, and Y. Ishikawa. 2018. Conservation and lineage-specific rearrangements in the GOBP/PBP gene complex of distantly related ditrysian Lepidoptera. PLoS One 13: e0192762.

Ye, Z.-F., X.-L. Liu, Q. Han, H. Liao, X.-T. Dong, G.-H. Zhu, and S.-L. Dong. 2017. Functional characterization of PBP1 gene in *Helicoverpa armigera* (Lepidoptera: Noctuidae) by using the CRISPR/Cas9 system. Sci. Rep. 7: 8470.

Yu, Y., P. Zhou, J. Zhang, C. Zheng, J. Zhang, and N. Chen. 2018. Pheromone-binding proteins in the Asian gypsy moth females, *Lymantria dispar*, recognizing the sex pheromone and plant volatiles. Arch. Insect Biochem. Physiol 99: e21477.

Zhang, S., Z. Zhang, H. Wang, and X. Kong. 2014. Antennal transcriptome analysis and comparison of olfactory genes in two sympatric defoliators, *Dendrolimus houi* and *Dendrolimus kikuchii* (Lepidoptera: Lasiocampidae). Insect Biochem. Mol. Biol 52: 69–81.

Zhang, L. W., K. Kang, S. C. Jiang, Y. N. Zhang, T. T. Wang, J. Zhang, L. Sun, Y. Q. Yang, C. C. Huang, L. Y. Jiang, et al. 2016. Analysis of the antennal transcriptome and insights into olfactory genes in *Hyphantria cunea* (Drury). PLoS One 11: e0164729.

Zhang, X. Y., X. Q. Zhu, S. H. Gu, Y. L. Zhou, S. Y. Wang, Y. J. Zhang, and Y. Y. Guo. 2017. Silencing of odorant binding protein gene *AlinOBP4* by RNAi induces declining electrophysiological responses of *Adelphocoris lineolatus* to six semiochemicals. Insect Sci. 24: 789–797.

Zhang, X. Q., Q. Yan, L. L. Li, J. W. Xu, D. Mang, X. L. Wang, H. H. Hoh, J. Ye, Q. Ju, Y. Ma, et al. 2020. Different binding properties of two general-odorant binding proteins in *Athetis lepigone* with sex pheromones, host plant volatiles and insecticides. Pestic. Biochem. Physiol 164: 173–182.

Zhou, J.-J. 2010. Odorant-binding proteins in insects. Vitamins and Hormones: Pheromones 83: 241–272.

Zhu, J., L. Ban, L. M. Song, Y. Liu, P. Pelosi, and G. Wang. 2016. General odorant-binding proteins and sex pheromone guide larvae of *Plutella xylostella* to better food. Insect Biochem. Mol. Biol 72: 10–19.

Zhu, G. H., M. Y. Zheng, J. B. Sun, S. A. Khuhro, Q. Yan, Y. Huang, Z. Syed, and S. L. Dong. 2019. CRISPR/Cas9 mediated gene knockout reveals a more important role of PBP1 than PBP2 in the perception of female sex pheromone components in *Spodoptera litura*. Insect Biochem. Mol. Biol 115: 103244.